Control of a multi-joint hand prosthesis – an experimental approach

Andrzej Wołczowski[1] and Janusz Jakubiak[1]

Wrocław University of Technology, Faculty of Electronics
Chair of Cybernetics and Robotics,
{Andrzej.Wolczowski|Janusz.Jakubiak}@pwr.edu.pl.

Abstract. The paper presents the concept of kinematic control of prosthetic hand with 13 d.o.f., while grasping objects of different shapes and sizes. The concept refers to the process of healthy hand motion control performed by the human nervous system. Planning of grip is based on kinematic model of the hand. The parameters of subsequent phases of the gripping process were determined experimentally from the measurements carried out with a laboratory model of hand. It was assumed that the final arrangement of fingers on the workpiece is determined on the basis of information from the touch sensor system.

Keywords: hand prosthesis, multi-joint structure control, gripping process

1 Introduction

Contemporary prosthetic hands are controlled in bioelectric manner - by recognition of user intention, expressed by myosignals (the signals associated with the muscles activity) from the stump of amputated limb. Such control is by the nature a two-level and two-stage process. At the first stage, the decision relating the type of the desirable prosthesis movement it is elaborated, and in the second stage the control of prosthesis mechanical structure (the motor control), performing this decision, is executed.

This control structure to a small extent maps multi-level process of hand movements control performed by the human nervous system [2, 5, 6]. In the central and peripheral nervous systems of human the flow of information is fully bidirectional: from the area of the motor cortex of the brain (where arises the motor decision), through the spinal cord and peripheral nerves, to the muscles motor end plates by efferent tracts, motor commands are transferred to muscles, whereas back: from the muscle activity receptors and sensory receptors in the skin of fingers leads the afferent tracts to the area of the sensory cortex. Sensory and motor areas of the cortex are frequently linked, allowing the control flow in a closed loop system. Also on the lower levels, information from afferent tract feedback (modifies) the efferent signals directed to the muscles, performing the reflex and stabilizing functions. This allows very precise control of the kinematic

structure (musculoskeletal structure) of hand and determines its unique dexterity. In comparison to the sensory system of natural hand the prosthesis sensory system, if it exists at all, is very poor, and control decisions defining the type of desirable motion, are necessarily limited to little numerous repertoire [7]. This causes that dexterity of today's active prostheses leaves much to be desired. A small step towards improving of their agility and flexibility, is to provide them in touch sensors, and to include this sensor information in the individual finger motor control in the process of grasping [3, 8].

The subject of the discussion of this article is the motor control capable of flexible execution of the prehensile/manipulation operations defined by movement decisions.

Experimental approach has been proposed based on the determination of the successive phases of prosthesis movement operation, based on measurements carried out on a laboratory model of a prosthetic hand. It was assumed that the final posture of fingers on the held object is fixed based on the touch feedback.

The organization of the paper is as follows. Section 2 presents the phases of the grasp. In section 3 the hardware setup is presented followed by kinematic analysis and proposed approach to the control in section 4. The preliminary tests results are presented in section 5 and summarized in section 6.

2 Model of grasping process

In the description of the grasping process we denote by A_F – finger posture, F_F – finger pressure force, V_F – finger velocity, V_A – velocity of arm movement, $V(2)$ – preceding stage velocity, K – human knowledge about the object being grasped (visual perception + experience), S – the sense of grab and arm movement.

In the process of grasping we can distinguish seven stages [6]:

1. rest position (starting point for the grasp preparation) – the fingers stay at rest position, are motionless and passive ($A_F \Leftarrow K$, V_F, $F_F = 0$),
2. grasp preparation (precedes grasp closing) – the fingers are arranged depending on the shape of visually observed object and the knowledge K about the method of gripping it, with the velocity proportional to the velocity of the intended arm movement ($A_F \Leftarrow K$, $V_F \sim V_A$),
3. grasp closing (precedes holding – the fingers move with the velocity resulting from the knowledge about the object and the arm velocity during the grasp preparation stage) $(V_F \Leftarrow K) \vee (V_F \sim V_A(2))$,
4. grabbing – the fingers press on the object with a force dependent on the knowledge of the object and proportionally to the arm motion velocity in the grasp preparation phase: $(F_F \Leftarrow K) \vee (F_F \sim V_A(2))$,
5. maintaining the grasp with force adjustment – the fingers adjust the force F_F depending on the amount of squeeze and slip of the object – increase/decrease the force ($F_F \sim S$),
6. releasing the grasp – the fingers move with a velocity dependent on the knowledge of the object behaviour (e.g. small V_F force for an object with an unstable balance): ($F_F \sim K$),

7. transition to the rest position – the fingers move with a constant velocity toward the rest position: ($V_F = \text{const}$),

Due to limitations in the exchange of information between the human nervous system and prosthesis control system (myosignals distortions and recognition process errors), the presented steps of the grasping process should be modified, replacing, as far as possible, central control by local control.

Prosthesis grasping process is as follows, with additional symbols meaning A_F^0 – the rest position, $y^\star$ – recognized user's decision, M – the measurement of grab parameters and arm movement.

1. rest position – fingers automatically take the rest setting A_F^0 stored in the control algorithm, remain stationary, passive ($A_F^0 \Leftarrow L$, V_F, $F_F = 0$),
2. grasp preparation – the type of grasp is defined by decision $y^\star$ from the user's intent recognition level (depending on the shape of visually observed object and the knowledge K about the method of gripping it), the hand opening is max for the type of object to be gripped, the velocity proportional to the velocity of the intended arm movement ($y^\star \Leftarrow K$, $A_F \Leftarrow A_F^{\max}(L)$, $V_F \Leftarrow M \vee V_F \sim V_A$),
3. grasp closing (precedes holding – the fingers move with the velocity resulting from the knowledge about the object and the arm velocity during the grasp preparation stage) ($V_F \Leftarrow K$) $\vee$ ($V_F \sim V_A(2)$),
4. grabbing – the movement of each finger member is stopped under the influence of information about touching the object to be gripped, the fingers touch/press on the object with a force established by decision $y^\star$ or proportionally to the arm motion velocity in the grasp preparation phase: ($F_F \Leftarrow K$) $\vee$ ($F_F \sim V_A(2)$),
5. maintaining the grasp with force adjustment – the fingers adjust the force F_F depending on the amount of squeeze and slip of the object – increase/decrease the force ($F_F \sim M$),
6. releasing the grasp – the fingers move with a velocity dependent on the knowledge of the object behaviour (e.g. small V_F force for an object with an unstable balance): ($F_F \sim K$),
7. transition to the rest position - the fingers move with a constant velocity toward the rest position: ($A_F, V_F \Leftarrow L$),

In this paper we concentrate on rest (1) to grabbing (4) phases.

3 Setup

Laboratory model of the hand prosthesis analyzed in this paper is presented in Fig. 1. An experimental setup consists of a mechanical hand built it our department by G. Wiśniewski and a computer application to send and receive control commands and to visualize hand configuration in GUI.

The mechanical hand is equipped with three fingers and a thumb. It has in total 16 rotational joints, out of which 13 are controlled independently. All

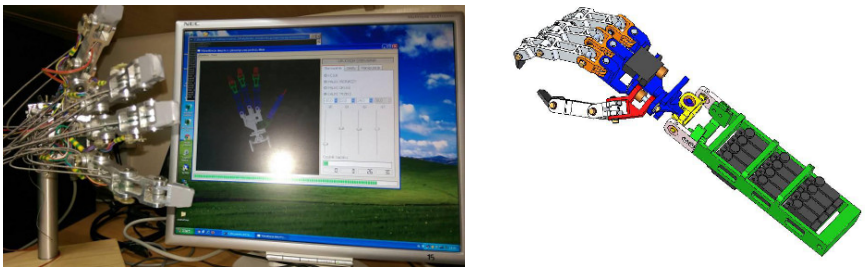

Fig. 1. Physical setup (left) and CAD model (right)

three fingers are identical with 4 joints and 3 d.o.f as the last two joints are coupled. The thumb has 4 independently controlled joints. Additional two rotational joints are placed in a wrist.

The prosthesis is actuated with 13 servo motors Futaba S3150. The one responsible for the thumb base rotation is placed in the palm and the remaining twelve – in the forearm. The servos input is PWM (pulse width modulation) signal with 20ms interval returning angle of the servo rotation as an output. The position of the shaft is transmitted to the joints with Bowden cables. The transmission ratio is 1:1, so the joint angle is proportional to the input signal.

All active joints of mechanical hand are equipped with a pulse encoders measuring their angular positions. Fingertips of thumb and index finger, and palm are equipped with force/touch sensors detecting when a digit is in contact with a grasped object.

4 Prosthesis control model

4.1 Kinematics

For the purpose of describing the kinematics of the hand, we treat it as a group of four maniplators mounted in different base points located on the palm, numbered from 0 to 3 where 0 denotes the thumb. To simplify notation, we assume that the origin O is in the base of finger 1, as shown in Fig. 2.

All digits are built in such a way that we can analyze them as two parts: a planar manipulator moving in plane Π_i and a rotating base which defines the orientation of the plane with respect to the palm. In the case of fingers the base rotation takes place in joint 1 and the remaining 3 joints move in a plane. In case of the thumb both base rotation and planar part include two joints. This observation allows us to simplify the analysis of the motion planning task by dividing them to two steps: analysis of digits' configurations in their planes and relations between the planes. A schematic plot in the palm plane is shown in Fig. 2.

We denote joint angles θ_{ij}, where i is the digit number and j – joint number counted from the palm (0) to the tip (3). All joint angles form a hand state

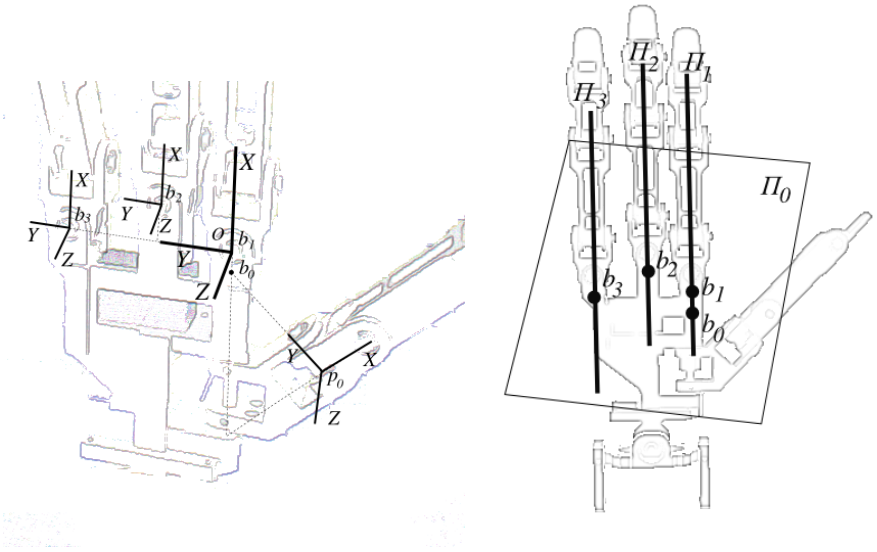

Fig. 2. Position and orientation of finger bases (left), finger motion planes (right)

$\theta = [\theta_{ij}]$, $i, j = 0, 1, 2, 3$. It is worth noticing that all planes associated with fingers are orthogonal to the palm, while the angle between the palm and the thumb plane Π_0 depends on the configurations of joints θ_{00} and θ_{01}.

Following the structure of the fingers, description of the kinematics of each digit will be divided in 3 parts

- constant transformation between the origin O and the base point of the finger b_i; it is worth noting that the points b_i are invariant points of plane Π_i rotations;
- transformation in the rotational base, between finger base b_i and planar part beginning p_i;
- transformation from p_i to the tip of digit e_i.

Coordinate transformations between X and Y consists of rotation R_X^Y and translation t_X^Y and will be represented as a standard homogeneous transformation A_X^Y [4]

$$A_X^Y = \begin{bmatrix} R_X^Y & t_X^Y \\ 0 & 1 \end{bmatrix},$$

with R_X^Y being 3×3 matrix and t_X^Y – 3 dimensional vector.

Transformations $A_O^{b_i}$ are constant and are defined by

$$R_O^{b_0} = \begin{bmatrix} 0 & 0 & 1 \\ 0 & -1 & 0 \\ -1 & 0 & 0 \end{bmatrix}, \qquad R_O^{b_i}|_{i=1,2,3} = I_3 \tag{1}$$

and

$$b_0 = \begin{bmatrix} -11.47 \\ 0 \\ 0 \end{bmatrix}, \quad b_1 = \begin{bmatrix} 0 \\ 0 \\ 0 \end{bmatrix}, \quad b_2 = \begin{bmatrix} 11 \\ 22 \\ 0 \end{bmatrix}, \quad b_3 = \begin{bmatrix} 0 \\ 49 \\ 0 \end{bmatrix}.$$

With the above definition of the base frames, the transformation between the base and the tip of each digit $A_{b_i}^{e_i}$ can be described with standard Denavit-Hartenberg parameters [1]. Kinematic parameters of the digits are given in Table 1. Note that for fingers the joints 2 and 3 are coupled, so the angle θ_{i2} in the

Table 1. Denavit-Hartenberg parameters

	fingers 1,2,3			
joint no.	θ	d	a	α
0	θ_{i0}	0	L_0	$\frac{\pi}{2}$
1	θ_{i1}	0	L_1	0
2	θ_{i2}	0	L_2	0
3	θ_{i2}	0	L_3	0

	thumb			
joint no.	θ	d	a	α
0	θ_{00}	0	0	$\frac{\pi}{4}$
1	θ_{01}	$-d_1$	L_1	$\frac{\pi}{2}$
2	θ_{02}	0	L_2	0
3	θ_{03}	0	L_3	0

left table is repeated.

A transformation between the origin and p_i is given by

$$A_O^{p_i} = A_O^{b_i} A_{b_i}^{p_i}$$

and together with point b_i it defines a plane in which the planar section of the digit i moves.

For the fingers, transformations $A_{b_i}^{p_i}$ and $A_O^{p_i}$ are defined by the configuration of joint 0

$$A_{b_i}^{p_i} = \begin{bmatrix} c_{i0} & 0 & s_{i0} & L_0 c_{i0} \\ s_{i0} & 0 & c_{i0} & L_0 s_{i0} \\ 0 & 1 & 0 & 0 \\ 0 & 0 & 0 & 1 \end{bmatrix} \qquad A_O^{p_i} = \begin{bmatrix} c_{i0} & 0 & s_{i0} & L_0 c_{i0} + b_{ix} \\ s_{i0} & 0 & c_{i0} & L_0 s_{i0} + b_{iy} \\ 0 & 1 & 0 & b_{iz} \\ 0 & 0 & 0 & 1 \end{bmatrix}. \tag{2}$$

The joints 1 to 3 form a triple pendulum moving in a plane defined by point b_i and the normal vector $\hat{n}_i$ from the third column of $R_O^{p_i}$

$$p_i = b_i + \begin{bmatrix} L_0 c_{i0} \\ L_0 s_{i0} \\ 0 \end{bmatrix}, \quad \hat{n}_i = \begin{bmatrix} s_{i0} \\ c_{i0} \\ 0 \end{bmatrix}, \quad \text{for } i = 1, 2, 3. \tag{3}$$

In case of the thumb the transformation between b_0 and p_0 is obtained as a product of transformations in the first two joints and it is given by

$$\begin{aligned} R_{b_0}^{p_0} &= \begin{bmatrix} c_{00}c_{01} - s_{00}s_{01}\frac{\sqrt{2}}{2} & s_{00}\frac{\sqrt{2}}{2} & c_{00}s_{01} + s_{00}c_{01}\frac{\sqrt{2}}{2} \\ s_{00}c_{01} - c_{00}s_{01}\frac{\sqrt{2}}{2} & -c_{00}\frac{\sqrt{2}}{2} & s_{00}s_{01} - c_{00}c_{01}\frac{\sqrt{2}}{2} \\ s_{01}\frac{\sqrt{2}}{2} & \frac{\sqrt{2}}{2} & c_{01}\frac{\sqrt{2}}{2} \end{bmatrix} \\ t_{b_0}^{p_0} &= \begin{bmatrix} -d_1 s_{00}\frac{\sqrt{2}}{2}, d_1 c_{00}\frac{\sqrt{2}}{2}, -d_1\frac{\sqrt{2}}{2} \end{bmatrix}^T \end{aligned} \tag{4}$$

After transformation to the global frame we obtain a plane in which the last two segments of the thumb move

$$p_0 = t_O^{p_0} = b_0 + t_{b_0}^{p_0}, \quad \hat{n}_0 = R_O^{p_0} \begin{bmatrix} 0 \\ 0 \\ 1 \end{bmatrix} = \begin{bmatrix} c_{01}\frac{\sqrt{2}}{2} \\ -s_{00}s_{01} + c_{00}c_{01}\frac{\sqrt{2}}{2} \\ -c_{00}s_{01} - s_{00}c_{01}\frac{\sqrt{2}}{2} \end{bmatrix}. \tag{5}$$

Note that the plane of thumb planar motion is orthogonal to the palm when $-c_{00}s_{01} - s_{00}c_{01}\frac{\sqrt{2}}{2} = 0$ and the planes Π_i and Π_j are parallel when $\hat{n}_i$ and $\hat{n}_j$ are.

4.2 Control of hand joints

During given grasp operation op_N joints are moved from an initial state $\theta^N(0)$ to a final configuration $\theta^N(k_N)$. Additional parameter of op_N is the grasp type which determines the planes in which the tips of digits move in the grasp closing phase. It is assumed that initial and final state and a grasp type are known and they are parameters of the grasping procedure, in the first approach it is also assumed that orientation of the planes depend on grasp type only and not on the initial and final state.

1. Joints 0 for fingers and 0 and 1 for thumb are set to proper angles with respect to the grasp type.
2. For the joint j of the finger i we determine a pair of angles describing its initial and final configurations $(\theta_{ij}(s_0), \theta_{ij}(s_N))$.
3. For each joint we determine desired displacement $\theta_{ij}(s_N) - \theta_{ij}(s_0)$.
4. We assume number of steps k to move to the requested configuration.
5. As a result we receive single-step change required in each joint in every

$$\Delta_{ij} = \frac{\theta_{ij}(s_N) - \theta_{ij}(s_0)}{k}$$

6. The single-state goals are than send to the joints to execute motion until one of conditions is met: the goal angle is reached or the touch sensor detects contact with the object as presented in Fig. 3. The step is repeated until all digits are in contact with the object or the minimum angle was reached.

5 Experiments

The experiments were divided in two parts. In the first one, the joint angles were measured in rest and grasp positions, for various grasp types and objects of various sizes. Tests covered cylindrical, hook, tip and lateral grasps.

During the motion operation the initial configuration $\theta(0)$ and the final configuration $\theta(k_N)$ were defined by the sets of angles in finger joints. The first set is defined for the rest configuration, the latter – for the destination grasp while handling the object.

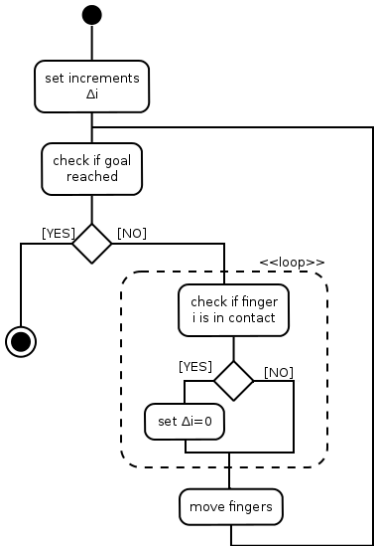

Fig. 3. Control scheme

In the experiments different types of object were handled and below we present two examples for different grasp types. The first example is a cylindrical grasp of a glass, the second is a tip grasp of a ball.

The angles in the hand rest position and grasps were collected in user supervised procedure. For chosen objects the user was properly placing the fingers to obtain stable grasp. Each finger was configured separately and its orientation angle was manually tuned. Next the obtained angles for an object were recorded as the grasp patterns for those objects. The results for examplary grasps are collected in Table 2.

Table 2. Joint angles in rest and grasp positions

	fingers											
	rest				cylindrical				tip			
joint no.	0	1	2	3	0	1	2	3	0	1	2	3
1	0	13	0	0	77	11	5	0	81	16	0	0
2	0	0	0	0	1	21	39	44	2	24	0	0
3	0	0	0	26	-9	58	64	55	-4	58	0	0
4	4	0	0	26	19	58	64	55	48	58	0	0

Based on the predefined initial and final state, the single-step change was determined with an assumption that the transfer from the rest configuration to the grasp is done in 2s. The maximum velocity of joints depends on finger and hand configurations. We determined empirically safe value for planning as $45°/s$.

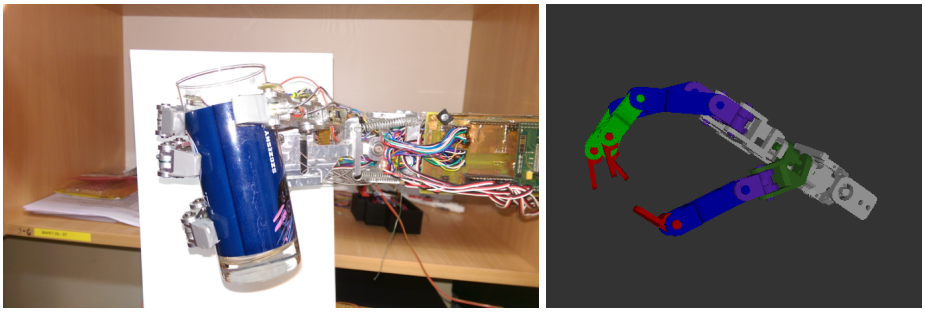

Fig. 4. A cylindrical grasp – virtual model and realization

That results in dividing the task into $k = 10$ steps. The results of planning are presented in the Table 3 to the left. To the right we show the results of exemplary experiments for each grasp. The motion time was $2.07s$ for the cylindrical and $1.83s$ for the tip grasp. In the table we put the average velocities of the motion. It can be noted that the time of real motion differs slightly from the planned and may be either shorter or longer than planned $2s$.

Table 3. Planned single-step angle change for $k = 10$ and measured average velocity

	planned increments °/step						measured avg. velocity °/s					
	cylindrical				tip		cylindrical				tip	
joint no.	0	1	2	3	0	1	0	1	2	3	0	1
1	7.7	-0.2	0.5	0	8.1	0.3	37	-1	2	0	44	2
2	0.1	2.1	3.9	4.4	0.2	2.4	0.5	10	19	21	1	13
3	-0.9	5.8	6.4	2.9	-0.4	5.8	-4	28	31	14	-2	32
4	1.5	5.8	6.4	2.9	4.4	5.8	7	28	31	14	24	32

Configuration of the fingers during cylindrical and tip grasps for virtual model and real hand are presented in Fig. 4 and 5.

6 Conclusions

Experiments has shown that with the proposed method it is possible to achieve sure grasp and handling of objects with different shapes and dimensions.

The objects used in the experiments were rigid and light. Apart from the grasp envelope and velocity, also the applied force influences grip safety. In the experiments touch and handling force was set to the level which ensures nonslip grip of the handled object. The proposed algorithm allows defining maximum value of grasp force. When detected force is bigger than predefined maximum, the closing motion of hand fingers is stopped. In future it is possible to define higher level layer which would allow passing to the phase of maintaining the

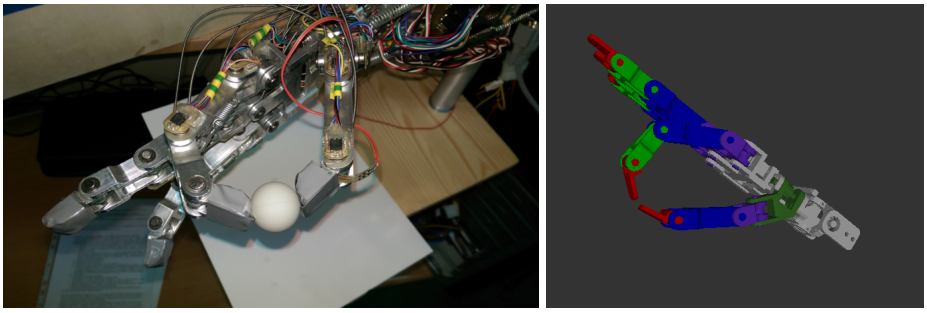

Fig. 5. A tip grasp – virtual model and realization

grasp. In that phase the force limit could be increased on demand to correct the grasp with a visual supervision of the user and disallow object to slip out. Non-slippery function can also be automated by additional slip sensors, what will be the subject of further research.

Acknowledgements

The work of the first author was supported by National Science Center resources in 2012-2014 years as a research project No. ST6/06168. The work of the second author was supported by statutory grant No. S40142. Computational resources were provided by PL-Grid Infrastructure.

References

1. Denavit, J., Hartenberg, R.S.: A kinematic notation for lower-pair mechanisms based on matrices. Trans. of the ASME. Journal of Applied Mechanics 22, 215–221 (1955)
2. Iberall, A.: A neural model of human prehension. Tech. rep., University of Massachusetts (1987)
3. Kurzynski, M., Wolczowski, A.: Control system of bioprosthetic hand based on advanced analysis of biosignals and feedback from the prosthesis sensors. In: E. Pietka, J.K. (ed.) Information Technologies in Biomedicine,, LNCS, vol. 7339, pp. 199–208. Springer, Berlin-Heidelberg (2012)
4. Sciavicco, L., Siciliano, B.: Modelling and Control of Robot Manipulators. The McGraw-Hill, New York (1996)
5. Taylor, C., Schwarz, R.: The anatomy and mechanics of the human hand. Artificial Limbs (2), 22–35 (1955)
6. Wołczowski, A.: Smart hand: the concept of sensor based control. In: Proceedings of MMAR. pp. 783–790. Miedzyzdroje (2001)
7. Wolczowski, A., Kurzynski, M.: Human-machine interface in bioprosthesis control using emg signal classification. Expert Systems 27(1), 53–70 (2010)
8. Wolczowski, A., Kurzynski, M., Zaplotny, P.: Concept of a system for training of bioprosthetic hand control in one side handless humans using virtual reality and visual and sensory biofeedback. J Med Infor & Tech 18, 85–91 (2011)